frontiers | Frontiers in Thermal Engineering

ORIGINAL RESEARCH
published: 29 June 2022
doi: 10.3389/fther.2022.905015

Improving Cooling Capacity of Condensation-Free Radiant Cooling for Low-Emissivity Chilled Ceiling *via* Adaptive Double-Skin Infrared Membranes

Ke Du[1,2], *Huijun Wu*[1,2]*, *Yanling Guo*[1,2], *Gongsheng Huang*[3], *Xinhua Xu*[4] *and Yanchen Liu*[1,2]

[1]School of Civil Engineering, Guangzhou University, Guangzhou, China, [2]Guangdong Provincial Key Laboratory of Building Energy Efficiency and Application Technologies, Guangzhou University, Guangzhou, China, [3]Department of Architecture and Civil Engineering, City University of Hong Kong, Hong Kong, China, [4]Department of Building Environment and Energy Engineering, Huazhong University of Science and Technology, Wuhan, China

OPEN ACCESS

Edited by:
Moran Wang,
Tsinghua University, China

Reviewed by:
Yudong Xia,
Hangzhou Dianzi University, China
Guangcai Gong,
Hunan University, China
Xin Cui,
Xi'an Jiaotong University, China

***Correspondence:**
Huijun Wu
wuhuijun@tsinghua.org.cn

Specialty section:
This article was submitted to Advancements in Cooling and Heating, a section of the journal Frontiers in Thermal Engineering

Received: 26 March 2022
Accepted: 13 May 2022
Published: 29 June 2022

Citation:
Du K, Wu H, Guo Y, Huang G, Xu X and Liu Y (2022) Improving Cooling Capacity of Condensation-Free Radiant Cooling for Low-Emissivity Chilled Ceiling via Adaptive Double-Skin Infrared Membranes. Front. Therm. Eng. 2:905015. doi: 10.3389/fther.2022.905015

Radiant cooling has well been acknowledged as energy efficient and thermal comfortable technology compared to conventional convective cooling. However, the radiant cooling exists two serious problems (viz., insufficient cooling capacity and high condensation risk) especially in hot and humid climate zones. By adding double-skin infrared transparent membranes (DIMs) onto radiant cooling panel, the air-contact surface can be separated from the cooling source surface, which makes it possible to use a low-temperature cooling source while maintaining air-contact surface higher than dew point temperature. The DIMs are transparent to radiant heat transfer which yields great cooling capacity while chilled ceiling has high emissivity (e.g., above 0.9). However, for metal chilled ceilings having low emissivity, radiant heat from cooling load to chilled ceiling would be reduced through DIMs, which results in insufficient cooling capacity. In this paper, a type of adaptive double-skin infrared membranes (a-DIMs) consisting a high-emissivity membrane and a high transparent membrane is proposed to improve cooling capacity of conventional metal chilled ceilings. The high-emissivity membrane serves as radiant cooling surface instead of low-emissivity chilled ceiling so as to improve radiant heat flux, while the high transparent membrane permits great radiant heat from cooling load to chilled ceiling. A combined heat transfer analysis based on semi-transparent surface radiation and natural convection were carried out to predict cooling capacity of condensation-free radiant cooling. The results indicate that the cooling capacity could be up to 101.9W/㎡ by adding a-DIMs consisting of a high-emissivity membrane of 0.96 and a high transparent membrane of 0.87, which is improved by 2 times compared to conventional metal chilled ceiling with low emissivity of 0.2. Moreover, the cooling capacity by adding a-DIMs is further improved by 25% compared to that by using both infrared transparent DIMs presented in our previous work. The results also indicate that the cooling capacity could be improved by above 2 times compared to conventional low-emissivity metal chilled ceiling by using the radiant cooling with a-DIMs for various humidity. It will be of great guidance for high-performance

radiant cooling design without condensation and improved cooling capacity for low-emissivity metal chilled ceiling.

Keywords: radiant cooling, condensation-free, cooling capacity, infrared radiative properties, DIMs

1 INTRODUCTION

The rapid urbanization has promoted growth in the economic development and also led to the rapid rise in the proportion of building energy consumption in the total energy expenditure in China (Xu et al., 2016). The report (Building energy saving research center of Tsinghua University, 2020) in 2020 shows that the energy consumption of construction operation accounts for about 22% of the total energy consumption of the society in China, for which the demand of energy saving on construction operation is urgent. Indoor cooling is one of main reasons for the increase of building energy consumption (Shan et al., 2017). Compared with conventional air-conditioning systems, radiant cooling has been verified to have many advantages (Rhee and Kim, 2015), including energy conservation (Niu et al., 2002; Hassan and Abdelaziz, 2020; Li et al., 2020), thermal comfort (Tian and Love, 2008; Kim et al., 2018; Karacavus and Aydin, 2019), and indoor air quality (Jagjit et al., 2010; Saber et al., 2014). However, due to the restriction of dew point temperature on cooling source temperature (Wu et al., 2021), the cooling capacity was limited, which hindered the application of radiant cooling in hot and humid areas (Rhee et al., 2017; Ning, 2020).

In order to overcome the limitation of the dew point temperature on the cooling capacity of the radiant cooling, a kind of infrared-transparent membranes was used to separate the radiant cooling surface from the ambient air. It provides possibility to improve cooling capacity by reducing the temperature of the cooling source while maintaining air-contact surface temperature above dew-point temperature for condensation-free purpose. This method was first proposed by Morse (Morse, 1963) in the 1960s and recently validated by (Teitelbaum et al., 2019) by selecting several commonly used polymer materials as infrared transparent membranes. The experiments showed that a low temperature cooling source of 5°C could be adopted in a 32°C/70% RH environment without condensation, where the effective radiant temperature for cooling was 15.8°C. Also, (Teitelbaum et al., 2020) constructed an outdoor radiation-cooling pavilion that used an infrared-transparent membrane to provide radiant cooling at temperatures below the dew point. The work demonstrated the feasibility of infrared membranes to improve radiant cooling capacity by using low temperature cooling source below dew-point.

Very recently, quantitative evaluation of radiant cooling with infrared transparent membranes on cooling capacity was carried out by numerical modelling and reduced-scale experiments. (Xing et al., 2020) established a performance prediction model for the radiant cooling with an infrared transparent membrane to predict cooling capacity. By using the model, the effect of infrared transparent membrane properties on cooling capacity an infrared transparent cover was also investigated. The results showed that the temperature of the radiant cooling surface could be lowered to 7°C without condensation under relative humidity below 65%. The corresponding cooling capacity was 103.2W/㎡, which improved by 42% compared with conventional radiant cooling. (Liang et al., 2021). developed a computational fluid dynamic model to evaluate the thermal environment of radiant cooling using low cooling temperature. And the results indicated that the thermal comfort under low radiant cooling temperature satisfied the comfort criteria of ASHRAE Standard. (Zhang et al., 2021). established a heat transfer model using a two-flux method for air-layer integrated radiant cooling unit, which in return can help the selection or specify criteria for the development of materials for the infrared-transparent membrane. (Du et al., 2021). proposed a condensation-free radiant cooling by covering cooling source with double-skin infrared-transparent membranes (DIMs). The relevant heat transfer model and reduced-scale experiment was carried out so as to demonstrate cooling capacity improvement. The results indicated that the cooling capacity with DIMs could be up to 104.0 W/㎡, 48% improved compared to conventional radiant cooling by using low temperature cooling source of 7°C. Meanwhile, the risk of condensation was eliminated by controlling the air-contact surface temperature higher than the dew point temperature. Therefore, adding infrared transparent membranes onto chilled ceiling provide possibility to use a low-temperature cooling source while maintaining air-contact surface higher than dew point temperature so as to improve cooling capacity.

The previous literature on infrared membranes assisted radiant cooling focused on chilled ceiling with high emissivity, e.g., 0.95 (Teitelbaum et al., 2019), 0.9 (Xing et al., 2020), 0.95 (Du et al., 2021). High emissivity chilled ceiling has great radiant potential from cooling load to cooling source, where infrared transparent membrane is advantageous to sufficient cooling capacity. However, chilled chilling can be categorized into two types according to the radiative properties of the surface (Li et al., 2008). One has a high emissivity surface (e.g., the chilled water tubing was directly embedded in the structural slabs, gypsum board, or plaster, which serves as the cooling surface, and the emissivity of these materials is generally higher than 0.9). The other has a low emissivity surface [e.g., suspended metal ceiling panels with copper tubing, in order to reduce heat transfer resistance, are generally made of aluminum, iron and other metal materials with emissivity of about 0.2–0.3 (Lu, 2020)]. Concerning the latter low eimissivity chilled ceiling, radiant potential from cooling load to chilled ceiling would be reduced, which results in insufficient cooling capacity. Herein, infrared transparent membrane covering chilled ceiling may be not optimized for improving cooling capacity. The cooling capacity can be further improved by optimizing infrared parameters of infrared membrane assisted radiant cooling.

In this work, in order to improve the cooling capacity of the metal chilled ceiling, which is greatly limited due to its

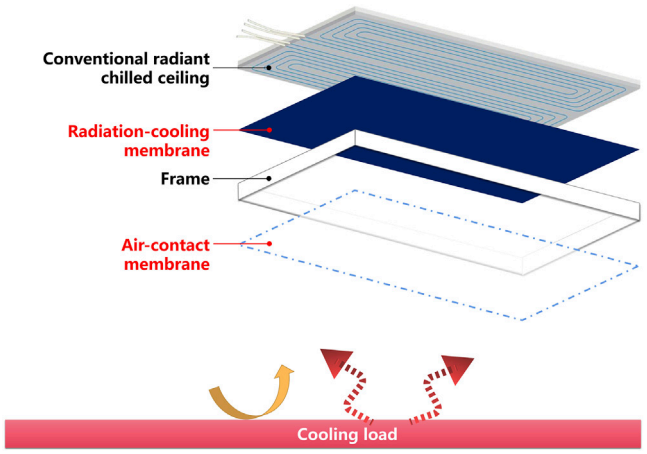

FIGURE 1 | Structure of condensation-free radiant cooling with a-DIMs.

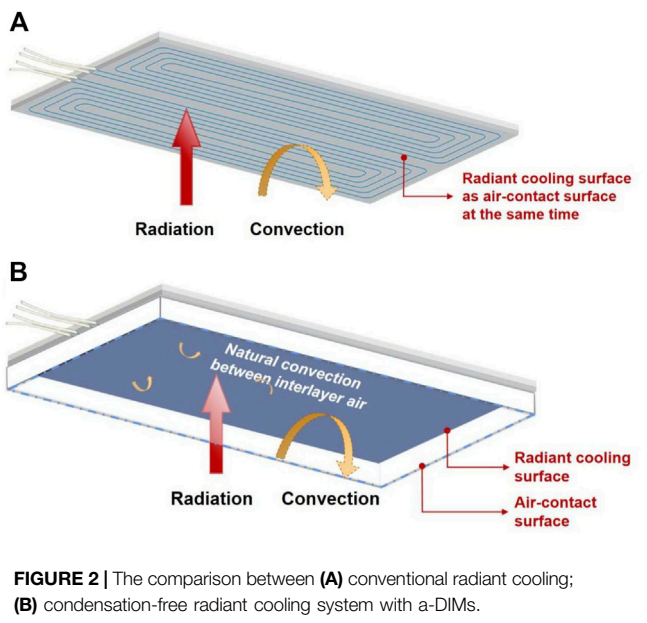

FIGURE 2 | The comparison between **(A)** conventional radiant cooling; **(B)** condensation-free radiant cooling system with a-DIMs.

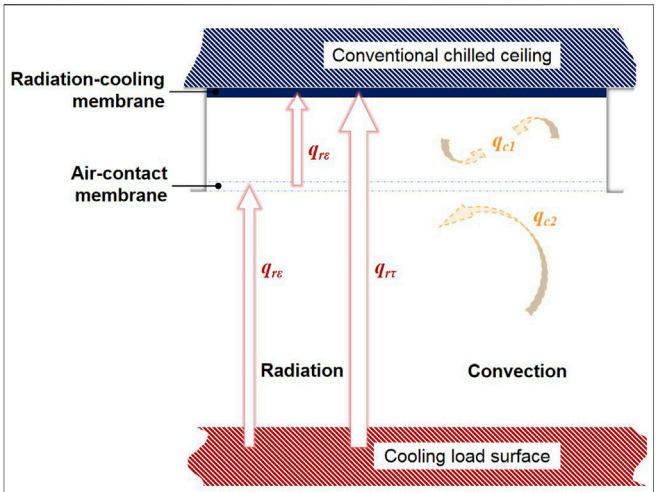

FIGURE 3 | Overall heat transfer process of condensation-free radiant cooling with a-DIMs.

low-emissivity surface, a type of adaptive double-skin infrared membranes (a-DIMs) consisting a high emissivity membrane and a high transparent membrane was proposed. A heat transfer model of condensation-free radiant cooling with a-DIMs was established. The effect of infrared membranes and interlayer of a-DIMs on the cooling performance was explored under the condensation-free conditions.

2 Modelling of Condensation-free Radiant Cooling With A-DIMs

Figure 1 gives the structure of condensation-free radiant cooling with a-DIMs. It consists of the chilled ceiling, the upper infrared (IR) membrane, frame, interlayer air and lower IR membrane. The upper IR membrane, which adheres to the surface of the chilled ceiling, has little thermal resistance due to the small thickness (about 50 μm). Therefore, some hypotheses were proposed. The temperature of the upper IR membrane is equal everywhere on the surface and to that of the cooling source. The temperature of the upper IR membrane can be approximated as the cooling temperature and its lower surface replaces the surface of chilled ceiling as radiant cooling surface. Thus, the upper IR membrane is functionally named as the radiation-cooling membrane. The lower IR membrane separates ambient air from the interlayer air formed by a-DIMs, and the lower surface of the membrane serves as the air-contact surface, so that the lower IR membrane is functionally named as the (ambient) air-contact membrane.

The upper and lower IR membranes were sealed and filled with dry air in the middle to form the double-skin IR membranes, which decomposed the two targets of improving cooling capacity and preventing condensation. For conventional radiant cooling, the cooling source surface serves as the air-contact surface at the same time as **Figure 2A**. However, for the radiant cooling with a-DIMs, the air-contact and radiant surfaces are decoupled by the a-DIMs, as **Figure 2B**. In this structure, the infrared transparency of the membrane allows radiant heat exchange occurring directly between the radiant cooling and the radiant load, whereas the dry air layer with low-thermal conductivity is able to maintain a high air-contact surface temperature, leading to a high reliability of condensation prevention. The radiation-cooling membrane can improve the cooling capacity by reducing the cooling temperature. And the air-contact membrane can avoid condensation by maintaining its temperature higher than the dew point temperature of ambient air. When both the upper and lower IR membranes have high transmittance, these are called double-skin infrared-transparent membranes (DIMs) (Du et al., 2021). In this work, aiming at improving cooling capacity of low-emissivity metal chilled ceiling, a new type of adaptive double-skin infrared

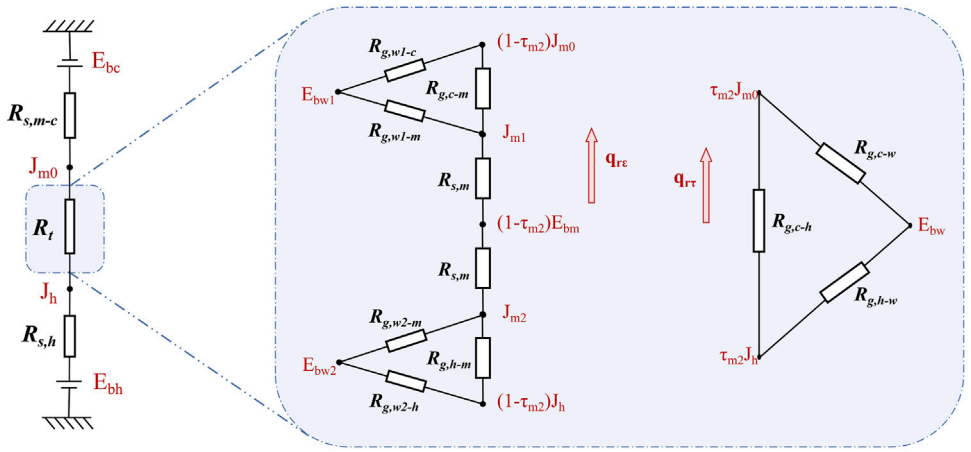

FIGURE 4 | Radiation network representing net radiation transfer between cooling surface and cooling load surfaces.

membranes (a-DIMs) consisting of one layer of high-emissivity radiation-cooling membrane and one layer of high-transmittance air-contact membrane are proposed.

As shown in **Figure 3**, the cooling capacity of the condensation-free radiant cooling with a-DIMs involves two parts, which can be expressed as:

$$q_t = q_r + q_c \tag{1}$$

where q_r is the radiant flux and qc is the convective flux. The convective flux is the convective heat transfer of interlayer dry air between the radiation-cooling surface and the air-contact surface. According to literature (Jack and John, 2011), the convective flux can be expressed as:

$$q_c = Nu \cdot \frac{\lambda}{\delta} \cdot \Delta T \tag{2}$$

where Nu λ is the thermal conductivity which depend on the mean temperature of interlayer air, δ is the thickness of the interlayer air of the a-DIMs, and ΔT is the temperature difference between the cooling source surface and the air-contact surface. Nu is the Nusselt number, which is a function of the Grashof number (Gr) and the Prandtl number (Pr). The values of Pr depend on the mean temperature of interlayer air, and

$$Gr = \frac{g\alpha \cdot \Delta T \cdot \delta^3}{\nu^2} \tag{3}$$

where g is the gravitational constant (9.81 m/s^2), α is the thermal diffusivity of the interlayer air, and ν is the dynamic viscosity of the interlayer air. Based on these values,

$$Nu = 1 \text{ for } \mathrm{Gr} \bullet \mathrm{Pr} \le 1700 \tag{4}$$

$$Nu = 0.059\,(Gr \cdot \mathrm{Pr})^{0.4} \text{ for } 1700 \le \mathrm{Gr} \bullet \mathrm{Pr} \le 7000 \tag{5}$$

$$Nu = 0.212\,(Gr \cdot \mathrm{Pr})^{0.25} \text{ for } 7000 \le \mathrm{Gr} \bullet \mathrm{Pr} \le 32000 \tag{6}$$

Figure 4 shows a radiation network representing the net radiation transfer between the cooling surface and cooling load surfaces. The radiant flux between the lower surface of the radiation-cooling membrane and the cooling load surface can be divided into two parts. The first is $q_{r\varepsilon}$ which is the radiation heat transfer participated by the air-contact membrane, which can be regarded as the radiation exchange through an opaque radiation shield. The second part is $q_{r\tau}$ which is the transparent radiant flux transferred between cooling source and cooling load.

The total radiant thermal flux through the membranes between the cooling load and the cooling source surface covering with an infrared-transparent membrane are characterized by the serial thermal resistance as shown in **Figure 4**. The black-body emissive powers associated with the temperature of each surface are connected to the radiosity nodes, using the appropriate form of the surface resistance. Hence, the net radiation exchange between the cooling source and cooling load may be expressed as:

$$q_r = \frac{E_{bh} - E_{bc}}{R_{s,m-c} + R_t + R_{s,h}} \tag{7}$$

where E_{bh} is the black-body emissive power of the cooling load surface, E_{bc} is black-body emissive power of the cooling source, $R_{s,m\text{-}c}$ is the surface radiant resistance of the infrared-transparent membrane when the diffused gray surface is used as the substrate, $R_{s,h}$ is the surface radiant resistance of cooling load surface, R_t is a multi radiant resistance. The radiant resistance of each part are calculated as follows:

$$R_{s,m-c} = \frac{\rho_{m1} + \rho_c \tau_{m1}}{\varepsilon_{m1} + \varepsilon_c \tau_{m1}} \tag{8}$$

$$R_t = \left((1-\tau_{m2}) \cdot R_{t\varepsilon}^{-1} + \tau_{m2} \cdot R_{t\tau}^{-1}\right)^{-1} \tag{9}$$

$$R_{s,h} = \frac{1-\varepsilon_h}{\varepsilon_h} \tag{10}$$

$$R_{t\varepsilon} = R_{s,c-m} + R_{s,m} + R_{s,m} + \left(R_{g,h-m}^{-1} + \left(R_{g,w-m} + R_{g,w-m}\right)^{-1}\right)^{-1} \tag{11}$$

$$R_{t\tau} = \left(R_{g,c-h}^{-1} + \left(R_{g,c-w} + R_{g,h-w}\right)^{-1}\right)^{-1} \tag{12}$$

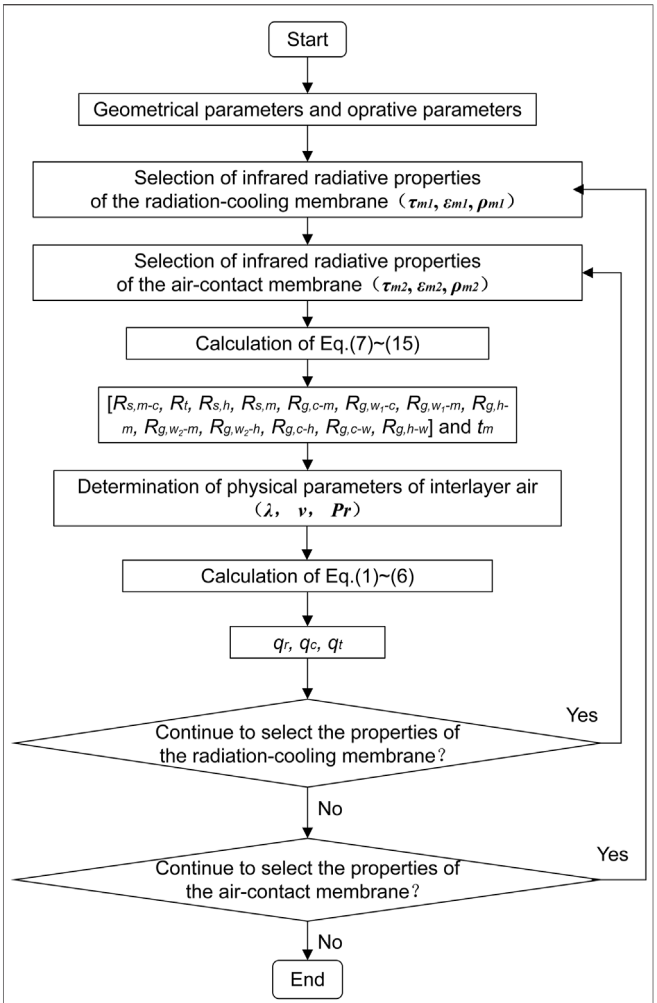

FIGURE 5 | Flowchart of numerical calculation.

$$R_{s,m} = \frac{\rho_{m2}}{\varepsilon_{m2}} \tag{13}$$

where ε, ρ and τ represent the emissivity, reflectivity and transmittance of a surface, respectively. The subscript *m1* represents the radiation-cooling membrane, the subscript *m2* represents the air-contact membrane, the subscript *h* represents the cooling load surface, and the subscript *c* represents the cooling source surface. R_g is the geometrical radiant resistance which is determined by the view factor between the surfaces, and R_s is the surface radiant resistance which is determined by the infrared radiative properties of the certain surface. The temperature of air-contact surface t_m can be calculated by the black-body emissive power of the air-contact membrane E_{bm}:

$$E_{bm} = J_{m0} + \frac{q_{r\varepsilon}\left(R_{s,m} + R_{g,c-m}\right)}{1 - \tau_{m2}} \tag{14}$$

$$t_m = \sqrt[4]{E_{bm}/\sigma} - 273.15 \tag{15}$$

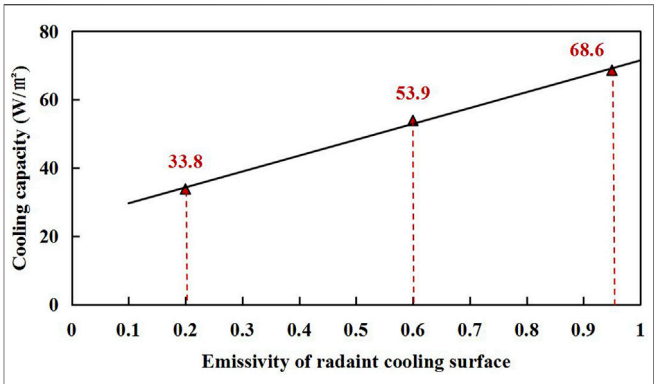

FIGURE 6 | The cooling capacity of the chilled ceiling with different emissivity surfaces when the radiant cooling temperature is set at 17.5.

where J_{m0} is the net radiation on the surface of the radiation-cooling membrane, and σ is Stefan-Boltzman constant, which is 5.67×10^{8}.

The infrared radiative properties of the membranes, including emissivity, reflectivity and transmittance, are crucial to the cooling performance of condensation-free radiant cooling with a-DIMs. For various infrared radiative parameters, the cooling capacity (including radiant flux and convective flux) is calculated according to the above formulas. The effect of the radiative properties parameters of the radiation-cooling membrane and air-contact membrane on the cooling performance is studied. The numerical calculation is shown in **Figure 5**.

3 RESULTS AND DISCUSSION

3.1 Effect of the Emissivity of Radiant Cooling Surface on Cooling Performance

The common types used in the chilled ceiling include gypsum board, plaster, metal plate etc. The emissivity of these different surfaces is significantly different, and the radiant cooling capacity of bare chilled ceiling (without a-DIMs) is quite different, correspondingly. **Figure 6** shows the cooling capacity of the chilled ceiling with different emissivity surfaces when the radiant cooling temperature is set at 17.5°C. It can be observed that the cooling capacity decreased obviously as the radiant cooling temperature is reduced from 1.0 to 0.1. For instance, as the emissivity was preset at 0.95, 0.6 and 0.2, the cooling capacity was 68.6, 53.9 and 33.8W/㎡. For low-emissivity surface (such as 0.2 emissivity), the cooling capacity is only 0.62 times (0.8 emissivity) and 0.49 times (0.95 emissivity) of high-emissivity surface. The main reason is that the reduced emissivity of the radiant cooling surface weakens the radiant heat transfer between the cooling source and cooling load. Therefore, the cooling capacity of low-emissivity chilled ceiling is very poor, which is far from meeting the engineering requirement. And it is necessary to take measures to improve the cooling performance of low-emissivity chilled ceiling.

TABLE 1 | Parameters of infrared radiative properties of radiant-cooling and air-contact membranes.

	Condensation-free radiant cooling with DIMs			Condensation-free radiant cooling with a-DIMs		
	ε	τ	ρ	ε	τ	ρ
Radiation-cooling membrane	0.09	0.87	0.04	0.96	0	0.04
Air-contact membrane	0.09	0.87	0.04	0.09	0.87	0.04

TABLE 2 | Geometrical parameters and operating temperatures of radiant cooling with a-DIMs.

Thickness of interlayer	Size of radiant cooling chamber			Temperature of cooling load
δ (mm)	Length (mm)	width (mm)	Height (mm)	t_h (°C)
10	200	200	50	28

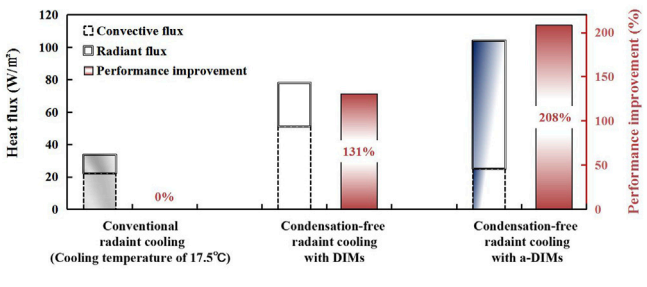

FIGURE 7 | Improvement of radiant cooling capacity with DIMs and a-DIMs compared to conventional low-emissivity chilled ceiling of 0.2.

3.2 Improving Cooling Capacity of Condensation-Free Radiant Cooling *via* Increasing the Infrared Radiative Properties of the Radiation-Cooling Membrane of the a-DIMs

An a-DIMs is used to solve the problem of poor performance of the low-emissivity chilled ceiling, which is critically related to the radiant-cooling membrane closely fitting with the surface of the chilled ceiling. Considering that the lower surface of radiation-cooling membrane replaces the surface of chilled ceiling as radiant cooling surface, it is analyzed to enhance the cooling capacity by increase the emissivity of the radiation-cooling membrane. Therefore, the high-emissivity membrane is selected as the radiation-cooling membrane. And the parameters of infrared radiative properties of the radiation-cooling membrane are shown in **Table 1**. The parameters of another membrane (air-contact membrane) are also given in **Table 1**. **Table 2** shows the geometrical parameters and operating temperatures of radiant cooling with a-DIMs. At the same time, in order to evaluate the suitability of DIMs to low-emissivity chilled chilling, two types of condensation-free radiant cooling are compared. The main difference between a-DIMs and DIMs is whether the radiation-cooling membrane has high transparency or emissivity.

Figure 7 shows the comparison of cooling capacity for low-emissivity chilled ceiling (0.2 emissivity) between conventional radiant cooling, radiant cooling with DIMs and radiant cooling with a-DIMs when the radiant cooling temperature was set at 8°C. In order to prevent condensation of ambient air, the air-contact surface temperature (t_m) should be controlled to be high than dew point temperature of ambient air (17.5°C for example). It can be calculated that the temperature of air-contact surface is 17.6°C using a-DIMs, and 23.5°C using DIMs, which are both higher than the dew point. Thus, the risk of condensation can be eliminated at a radiant cooling temperature of 8°C. The cooling capacity of radiant cooling with a-DIMs is 101.9W/㎡, which is improved by 2 times compared to conventional metal chilled ceiling with low emissivity of 0.2. Moreover, the cooling capacity by adding a-DIMs is further improved by 63% compared to that by using both infrared transparent DIMs.

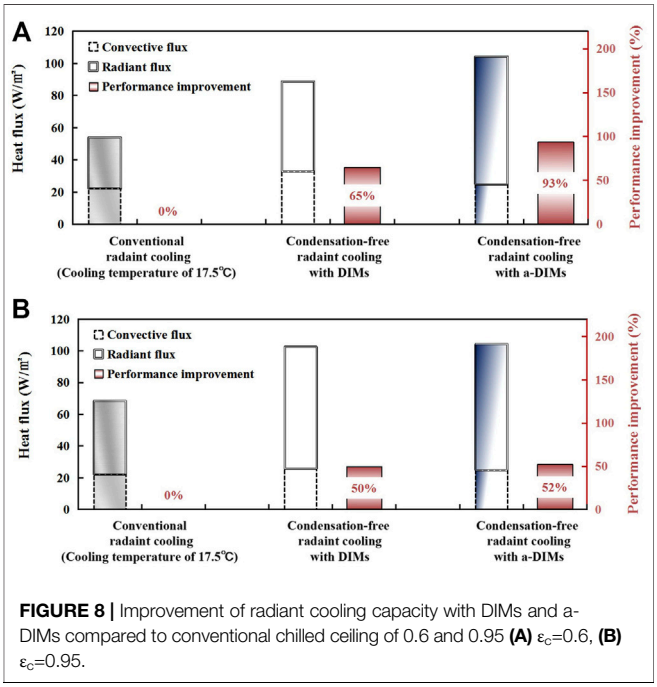

FIGURE 8 | Improvement of radiant cooling capacity with DIMs and a-DIMs compared to conventional chilled ceiling of 0.6 and 0.95 **(A)** ε_c=0.6, **(B)** ε_c=0.95.

In order to determine the suitability of the a-DIMs, **Figure 8** shows the comparison of cooling capacity of the chilled ceiling

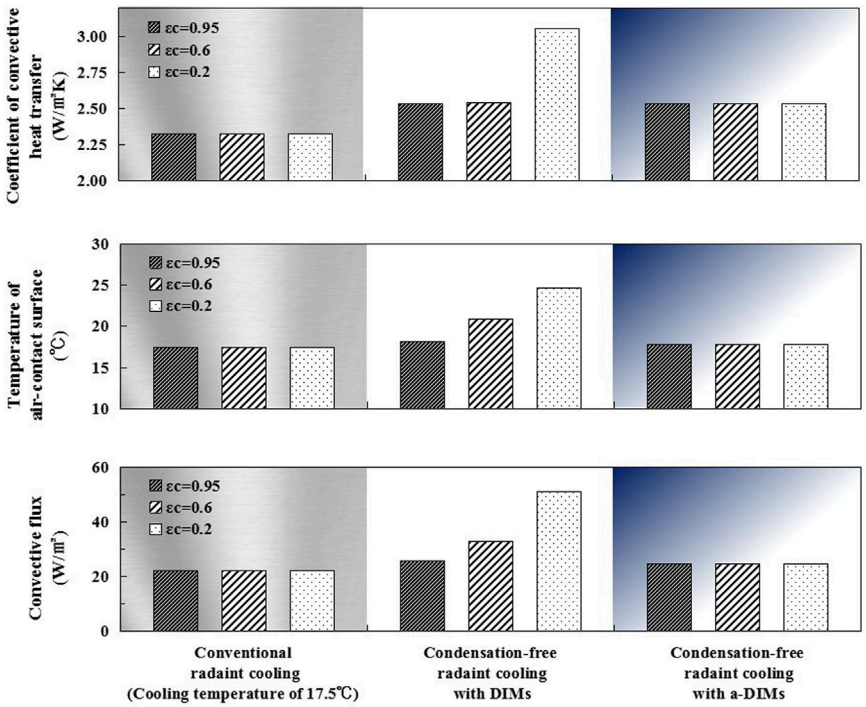

FIGURE 9 | Improvement of convective flux with DIMs and a-DIMs compared to conventional chilled ceiling with various emissivity of 0.2, 0.6 and 0.95.

with emissivity of 0.6 and 0.95, respectively. It can be observed that the cooling capacity of radiant cooling with a-DIMs is 104.3W/㎡for chilled ceilings with different emissivity, and the corresponding radiant flux and convective flux are the same. This is due to the high-emissivity radiation-cooling membrane takes place of the surface of chilled ceiling as radiant cooling surface to participate in the heat transfer process, thus the emissivity of the surface of chilled ceiling no longer affects the cooling performance. For conventional radiant cooling, the cooling capacity of the chilled ceiling with emissivity of 0.6 and 0.95 is 53.9 and 68.6 W/㎡, respectively. The cooling capacity of condensation-free radiant cooling with DIMs is increased by 65 and 50%, respectively, and that of condensation-free radiant cooling with a-DIMs is increased by 93 and 52%, respectively. Therefore, for the chilled ceiling with high-emissivity, radiant cooling with a-DIMs can also enhance the cooling capacity by reducing the radiant cooling temperature. And the improvement is better than radiant cooling with DIMs. However, the improvement is not as effective as for the chilled ceiling with low-emissivity.

It should be noted that, for the radiant cooling with a-DIMs, the maximum cooling capacity is achieved when the emissivity of the radiation-cooling membrane approaches 1.0. Moreover, in case of the transmittance of 0, the radiant characteristics of the original surface of chilled ceiling would not affect the cooling performance. When the emissivity of chilled ceiling is over 0.8, the cooling capacity improvement by using high-emissivity membrane is less than 5% compared with that by using high transparent membrane. Considering the low cost and easy availability of high transparent materials such as polyethylene, the DIMs is recommended. However, for the metal chilled ceiling with low emissivity, the cooling capacity of condensation-free radiant cooling with a-DIMs can be improved by 2 times. Moreover, the cooling capacity with a-DIMs can be further improved by 25% compared with DIMs.

Figures 7, **8** also show the radiant flux and convective flux included in the cooling capacity of two types of condensation-free radiant cooling. For the chilled ceiling with low-emissivity, the radiant flux of radiant cooling with a-DIMs is increased from 27.0W/㎡ to 79.5W/㎡ (2.9 times high) than that of radiant cooling with DIMs. The reason is that the radiation-cooling membrane with high-emissivity is selected, which greatly increases the radiant heat transfer on the cooling surface. However, it is obvious that the convective flux of radiant cooling with a-DIMs is reduced from 51.1W/㎡ to 24.8W/㎡ (2.1 times lower) compared with that of radiant cooling with DIMs.

To further investigate the reason why the convective flux of radiant cooling with a-DIMs is lower than that of radiant cooling with DIMs. **Figure 9** shows the comparison of the factors affecting convective heat transfer at different scenarios of radiant cooling. It can observed that, for the chilled ceiling with low-emissivity (such as 0.2 emissivity), the convective heat transfer coefficient and air-contact surface temperature of the radiant cooling with DIMs are much high than the values of the conventional radiant cooling and radiant cooling with

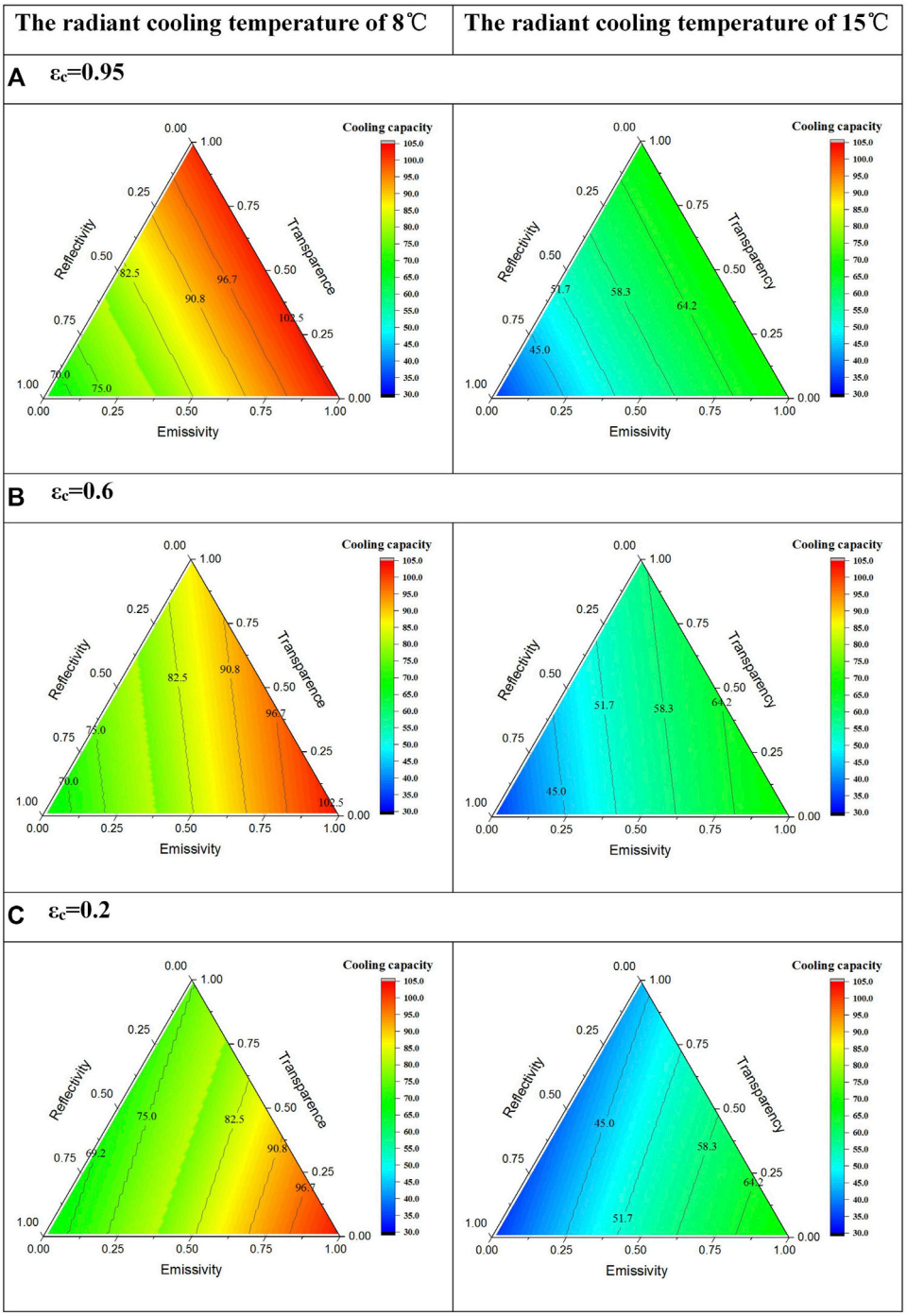

FIGURE 10 | Effect of the radiative properties parameters of the radiation-cooling membrane on the cooling capacity when the radiant cooling temperature set at 8 and 15.

a-DIMs. The main reason is that higher air-contact surface temperature can result in greater heat exchange temperature difference, higher average temperature as well as corresponding physical parameters of the interlayer air.

To further evaluate the effect of radiant cooling with a-DIMs, **Figure 10** shows the influence of the radiative properties parameters of the radiation-cooling membrane on the cooling capacity of the chilled ceiling with emissivity of 0.95, 0.6, and 0.2, respectively. It can be observed that the variation of cooling capacity with the radiative properties parameters of the radiation-cooling membrane is the same under different cooling temperature. For the chilled ceiling

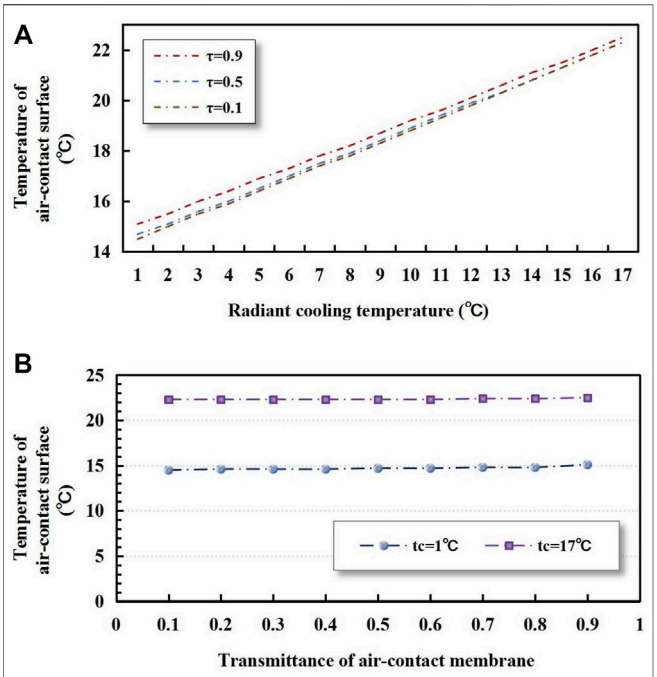

FIGURE 11 | Temperature of air-contact surface for various **(A)** radiant cooling temperature **(B)** transmittance of aircontact membrane.

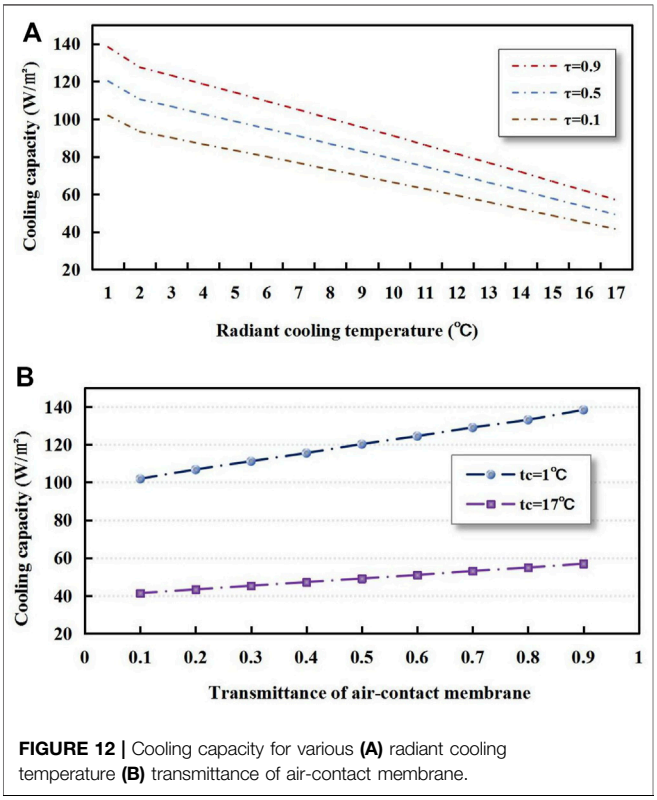

FIGURE 12 | Cooling capacity for various **(A)** radiant cooling temperature **(B)** transmittance of air-contact membrane.

with high-emissivity, the maximum cooling capacity occurs when the reflectivity of the radiation-cooling membrane is less than 0.05, with little effect of the transmittance or emissivity. For the chilled ceiling with low-emissivity, the maximum cooling capacity occurs when the emissivity of the radiation-cooling membrane approaches 1.0.

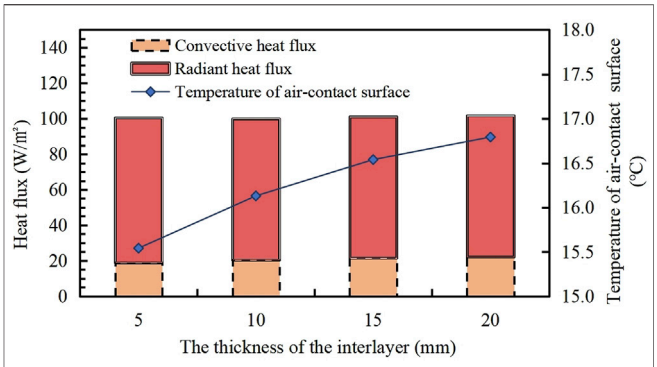

FIGURE 13 | Effect of interlayer thickness on cooling performance for radiant cooling temperature of 8°C.

3.3 Effect of Infrared Radiative Properties of Air-Contact Membrane on Cooling Capacity of Condensation-Free Radiant Cooling With a-DIMs

Figure 11 shows the temperature of air-contact surface of radiant cooling with a-DIMs for various radiant cooling temperature and transmittance of air-contact membrane. It can be observed that when the radiant cooling temperature increases from 1 to 17°C, the temperature of air-contact surface increase linearly. However, the change of air-contact surface temperature is slight with the increase of the transmittance of the air-contact membrane. For example, the change of air-contact surface temperatures are both within ± 0.1°C when the cooling temperature is set at 1 and 17°C. This indicates that the transmittance of air-contact membrane does not determine the condensation at an appropriate cooling temperature.

Figure 12 shows the cooling capacity of radiant cooling with a-DIMs for various radiant cooling temperature and transmittance of air-contact membrane. It can be observed that the cooling capacity increases as the radiant cooling temperature is decreased from 17 to 1°C. Moreover, the cooling capacity increases more rapidly when the cooling temperature decreases from 2 to 1. The reason is that the interlayer air changes from conduction to natural convection as the temperature difference increases. The convective flux and the cooling capacity increases as well. It can be also observed that when the transmittance of the air-contact membrane is improved from 0.1 to 0.9, the cooling capacity increases from 46.5 to 67.1W/m² at cooling temperature of 8°C, and increases from 46.5 to 67.1W/m² at cooling temperature of 15°C. In conclusion, with the increase of the transmittance, the temperature of the air-contact surface changes slightly and the cooling capacity increases significantly. Therefore, the transmittance as close as possible to 1.0 should be selected for the air-contact membrane.

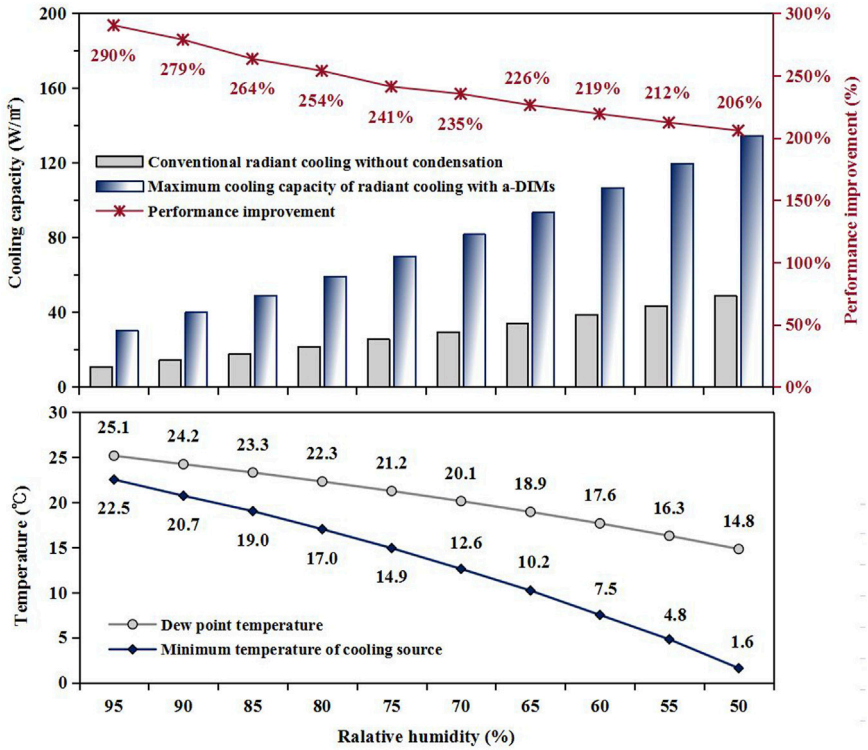

FIGURE 14 | Cooling capacity and performance improvement of condensation-free radiant cooling with a-DIMs under different RH conditions.

3.4 Effect of the Thickness of the Interlayer on the Cooling Performance

Figure 13 shows the effect of the interlayer thickness on the cooling performance when the radiant cooling temperature is set at 8°C. It can be observed that the temperature of air-contact surface increase from 15.5 to 16.8°C as the thickness of the interlayer is increased from 5 to 20 mm. However, the change of radiant and convective heat flux is slight with the variation of the thickness of the interlayer. This indicates that increasing the interlayer thickness can improve the safety of condensation-free radiant cooling with a-DIMs at the same cooling temperature.

3.5 Evaluating Cooling Performance of Condensation-Free Radiant Cooling With a-DIMs for Various Environmental Humidity

Humidity limits the cooling performance of radiant cooling by affecting the dew point temperature. For the conventional radiant cooling, the cooling temperature is not allowed below dew point of ambient air. On the other hand, under the condition that the air-contact surface temperature is controlled higher than the dew point temperature of ambient air, the cooling capacity of the condensation-free radiation cooling with a-DIMs can be increased by reducing the radiant cooling temperature, and the maximum cooling capacity can be obtained at the lowest allowable cooling temperature. **Figure 14** shows that the cooling capacity and the performance improvement of condensation-free radiant cooling with a-DIMs under different RH conditions and infrared radiative parameters of each surface as shown in **Table 3**. For instance, when the relative humidity is 75%, the corresponding dew point temperature is 21.2°C, and the lowest allowable cooling temperature can be set at 14.9°C. The maximum cooling capacity of radiant cooling with a-DIMs can reach 70.1W/㎡, 2.4 times performance improvement compared to conventional radiant cooling by using the cooling temperature of 21.2°C, which is equivalent to the dew point temperature. It can be observed that the cooling capacity of radiant cooling with a-DIMs decreases with the increase of relative humidity due to the augment of dew point temperature affected by RH. However, the performance improvement compared to conventional radiant cooling enhances with the increase of relative humidity. When the relative humidity is increased from 50 to 95%, the cooling capacity of radiant cooling with a-DIMs decreases from 134.5W/㎡ to 30.3W/㎡ and the performance improvement

TABLE 3 | Infrared radiative parameters of chilled ceiling surface and two layer infrared membranes.

	ε	τ	ρ
Chilled ceiling surface	0.2	0	0.8
Radiation-cooling membrane	0.96	0	0.04
Air-contact membrane	0.09	0.87	0.04

compared to conventional radiant cooling increases form 2.1 times to 2.9 times.

4 CONCLUSION

In order to solve the problem of insufficient cooling capacity of metal chilled ceilings with low emissivity, a new type of adaptive double-skin infrared membranes (a-DIMs) consisting of one layer of high-emissivity membrane and one layer of high transparent membrane is proposed in this paper. Compared with the conventional metal chilled ceiling with low emissivity of 0.2, the cooling capacity of condensation-free radiant cooling with a-DIMs can be improved by 2 times. Moreover, compared with double-skin infrared-transparent membranes (DIMs) presented in previous publication (Du et al., 2021), the cooling capacity with a-DIMs can be further improved by 25%. It is resulted from that high emissivity membrane in the a-DIMs was used to replace conventional metal low emissivity chilled ceiling and high transparent radiation cooling membrane in the previously presented radiant cooling with DIMs. The high emissivity radiation-cooling membrane in the a-DIMs significantly improved radiant heat flux from cooling load to cooling source.

For the radiant cooling with a-DIMs, the maximum cooling capacity is achieved when the emissivity of the radiation-cooling membrane approaches 1.0. Several kinds of carbon materials are feasible to be selected as the radiation-cooling membrane, which have been verified that the emissivity can reach more than 0.9. As for the air-contact membrane, the low-density polyethylene material could meet the infrared transparent requirement for the condensation-free radiant cooling with a-DIMs. However, high performance infrared-transparent membranes with high strength and air-tightness could be better choices, such as PE aerogels and infrared transparent inorganic ceramics.

Further investigations under various RH conditions demonstrated that significant improvement of cooling capacity above 2 times compared to conventional low-emissivity metal chilled ceiling by using the radiant cooling with a-DIMs. It will be of great guidance for high-performance radiant cooling design with condensation-free and improved cooling capacity especially for low-emissivity metal chilled ceiling.

DATA AVAILABILITY STATEMENT

The raw data supporting the conclusions of this article will be made available by the authors, without undue reservation.

AUTHOR CONTRIBUTIONS

Conception and design of study: HW, KD, GH, and XX Acquisition of data: KD Analysis and interpretation of data: KD, HW, and GH Drafting the manuscript: KD and HW Revising the manuscript critically for important intellectual content: HW, GH, XX, and YL Approval of the version of the manuscript to be published: KD, HW, YL, GH, XX, and YL.

FUNDING

This research was supported by the National Natural Science Foundation of China (No.52078144).

REFERENCES

Building energy saving research center of Tsinghua University (2020). *Annual Report on China Building Energy Efficiency*. Beijing: China Architecture and Building Press.

Du, K., Wu, H., Huang, G., Xu, X., and Liu, Y. (2021). Condensation-Free Radiant Cooling with Double-Skin Infrared-Transparent Membranes. *Build. Environ.* 193, 107660. doi:10.1016/j.buildenv.2021.107660

Hassan, M. A., and Abdelaziz, O. (2020). Best Practices and Recent Advances in Hydronic Radiant Cooling Systems–Part II: Simulation, Control, and Integration. *Energy Build.*, 110263. doi:10.1016/j.enbuild.2020.110263

Jack, P. H., and John, L. (2011). *Heat Transfer*. 10th. New York: McGraw-Hill.

Jagjit, S., Chuck, W., and Jeong, T. (2010). Building Pathology, Investigation of Sick Buildings - VOC Emissions. *Indoor Built Environ.* 19 (1), 30–39. doi:10.1177/1420326X09358799

Karacavus, B., and Aydin, K. (2019). Numerical Investigation of General and Local Thermal Comfort of an Office Equipped with Radiant Panels. *Indoor Built Environ.* 28 (6), 806–824. doi:10.1177/1420326x18799834

Kim, M. K., Liu, J., and Cao, S.-J. (2018). Energy Analysis of a Hybrid Radiant Cooling System Under Hot and Humid Climates: A Case Study at Shanghai in China. *Build. Environ.* 137, 208–214. doi:10.1016/j.buildenv.2018.04.006

Li, L., Zhao, L., and Meng, Q. (2008). Applicability Analysis on Ceiling Radiant Cooling with Displacement Ventilation System in Guangzhou. *Build. Sci.* (10), 74–78. doi:10.1007/s12273-020-0753-8

Li, Z., Zhang, D., Chen, X., and Li, C. (2020). A Comparative Study on Energy Saving and Economic Efficiency of Different Cooling Terminals Based on Exergy Analysis. *J. Build. Eng.* 30, 101224. doi:10.1016/j.jobe.2020.101224

Liang, Y., Zhang, N., Wu, H., Xu, X., Du, K., Yang, J., et al. (2021). Thermal Environment and Thermal Comfort Built by Decoupled Radiant Cooling Units with Low Radiant Cooling Temperature. *Build. Environ.* 206, 108342. doi:10.1016/j.buildenv.2021.108342

Lu, S. (2020). *Research on the Influence of Emissivity of Inner Surface of Envelope on Indoor Thermal Environment*. Guangzhou: South China University of Technology.

Morse, R. N. (1963). Radiant Cooling. *Archit. Sci. Rev.* 6 (2), 50–53. doi:10.1080/00038628.1963.9696068

Ning, B. (2020). A Radiant and Convective Time Series Method for Cooling Load Calculation of Radiant Ceiling Panel System. *Build. Environ.* 188, 107411. doi:10.1016/j.buildenv.2020.107411

Niu, J. L., Zhang, L. Z., and Zuo, H. G. (2002). Energy Savings Potential of Chilled-Ceiling Combined with Desiccant Cooling in Hot and Humid Climates. *Energy Build.* 34 (5), 487–495. doi:10.1016/s0378-7788(01)00132-3

Rhee, K.-N., and Kim, K. W. (2015). A 50 Year Review of Basic and Applied Research in Radiant Heating and Cooling Systems for the Built Environment. *Build. Environ.* 91, 166–190. doi:10.1016/j.buildenv.2015.03.040

Rhee, K.-N., Olesen, B. W., and Kim, K. W. (2017). Ten Questions About Radiant Heating and Cooling Systems. *Build. Environ.* 112, 367–381. doi:10.1016/j.buildenv.2016.11.030

Saber, E. M., Iyengar, R., Mast, M., Meggers, F., Tham, K. W., and Leibundgut, H. (2014). Thermal Comfort and IAQ Analysis of a Decentralized DOAS System

Coupled with Radiant Cooling for the Tropics. *Build. Environ.* 82, 361–370. doi:10.1016/j.buildenv.2014.09.001

Shan, H., Da, Y., and Guo, S. (2017). A Survey on Energy Consumption and Energy Usage Behavior of Households and Residential Building in Urban China. *Energy Build.* 148, 366–378. doi:10.1016/j.enbuild.2017.03.064

Teitelbaum, E., Chen, K. W., Aviv, D., Bradford, K., Ruefenacht, L., Sheppard, D., et al. (2020). Membrane-Assisted Radiant Cooling for Expanding Thermal Comfort Zones Globally without Air Conditioning. *Proc. Natl. Acad. Sci. U.S.A.* 117 (35), 21162–21169. doi:10.1073/pnas.2001678117

Teitelbaum, E., Rysanek, A., Pantelic, J., Aviv, D., Obelz, S., Buff, A., et al. (2019). Revisiting Radiant Cooling: Condensation-Free Heat Rejection Using Infrared-Transparent Enclosures of Chilled Panels. *Archit. Sci. Rev.* 62 (2), 152–159. doi:10.1080/00038628.2019.1566112

Tian, Z., and Love, J. A. (2008). A Field Study of Occupant Thermal Comfort and Thermal Environments with Radiant Slab Cooling. *Build. Environ.* 43 (10), 1658–1670. doi:10.1016/j.buildenv.2007.10.012

Wu, Y., Sun, H., Duan, M., Lin, B., and Zhao, H. (2021). Dehumidification-Adjustable Cooling of Radiant Cooling Terminals Based on a Flat Heat Pipe. *Build. Environ.* 194 (11), 107716. doi:10.1016/j.buildenv.2021.107716

Xing, D., Li, N., Cui, H., Zhou, L., and Liu, Q. (2020). Theoretical Study of Infrared Transparent Cover Preventing Condensation on Indoor Radiant Cooling Surfaces. *Energy* 201, 117694. doi:10.1016/j.energy.2020.117694

Xu, W., Sun, D., and Liu, Z. (2016). Performance Criteria System for Passive Nearly Zero Energy Buildings in China. *Indoor Built Environ.* 25 (8), 1181–1184. doi:10.1177/1420326x16674376

Zhang, N., Liang, Y., Wu, H., Xu, X., Du, K., Shao, Z., et al. (2021). Heat Transfer Modeling and Analysis of Air-Layer Integrated Radiant Cooling Unit. *Appl. Therm. Eng.* 194, 117086. doi:10.1016/j.applthermaleng.2021.117086

Conflict of Interest: The authors declare that the research was conducted in the absence of any commercial or financial relationships that could be construed as a potential conflict of interest.

Publisher's Note: All claims expressed in this article are solely those of the authors and do not necessarily represent those of their affiliated organizations, or those of the publisher, the editors and the reviewers. Any product that may be evaluated in this article, or claim that may be made by its manufacturer, is not guaranteed or endorsed by the publisher.

NOMENCLATURE

E Emissive power, W/㎡

G Incident radiant flux onto a surface, W/㎡

H Incident radiant flux across a medium, W/㎡

J Outgoing radiant flux from a surface, W/㎡

Q Energy per unit time, W

q Energy per unit area per unit time, W/㎡

R Thermal resistance, ㎡·K/W

T Absolute temperature, K

Nu Nusselt number hD/λ

Pr Prandtl number $c_p\mu/\lambda$

Greek Symbols

τ Transmittance of a medium

ε Emissivity of a medium

ρ Reflectivity of a surface

α Absorption of a medium

λ Thermal conductivity, W/(m·K)

Subscripts

b Blackbody condition

c Heat convection; Cold panel

h Hot panel

r Heat radiation

rτ Radiant energy resulting from transmittance

rε Radiant energy resulting from emissivity

t Total

m membrane

s Surface

g Geometrical

w Wall